A theoretical study of hydridocobalt carbonyls. II. Interdependence of geometry and electronic structure

Danko Antolovic and Ernest R. Davidson

Citation: The Journal of Chemical Physics **88**, 4967 (1988); doi: 10.1063/1.454708
View online: http://dx.doi.org/10.1063/1.454708
View Table of Contents: http://scitation.aip.org/content/aip/journal/jcp/88/8?ver=pdfcov
Published by the AIP Publishing

A theoretical study of hydridocobalt carbonyls. II. Interdependence of geometry and electronic structure

Danko Antolovic and Ernest R. Davidson
Department of Chemistry, Indiana University, Bloomington, Indiana 47405

(Received 5 March 1987; accepted 5 January 1988)

The electronic structure of hydridocobalt tri- and tetra-carbonyls was investigated by means of *ab initio* methods in two different Gaussian basis sets. Hartree–Fock, configuration-interaction, and MCSCF calculations were performed on a number of conformations and electronic states of both compounds. Pyramidal distortions of the symmetric C_{3v} forms of $HCo(CO)_3$ were investigated, and Jahn–Teller distortions of the triplet states were described at the MCSCF level of theory. The interdependence of correlation effects and molecular geometry was examined in both basis sets. It is concluded that dispersion forces play a large role in metal–ligand bonding and need to be included in the qualitative model.

INTRODUCTION

In an earlier article[1] (referred to as paper I), we reported the results of Hartree–Fock calculations of the geometry and electronic structure of hydridocobalt tri- and tetra-carbonyls. The present article gives an account of some further results, obtained primarily by the configuration-interaction and MCSCF methods with an enlarged basis set, regarding the electronic structure of the same compounds.

Geometry optimizations at the Hartree–Fock computational level have indicated the presence of two stable conformations of the $HCo(CO)_4$ compound, of C_{3v} and C_{2v} symmetry as well as several conformations of the closed-shell, singlet $HCO(CO)_3$. Moreover, a number of triplet configurations of the tricarbonyl, with different geometries, were described.

It is well known that the single-configuration methods provide an inadequate description of the compounds of transition metals.[2–7] The purpose of the present large-scale configuration-interaction calculations is to improve upon the description of conformations and electronic states of the cobalt complexes, whose optimized geometries were reported in paper I.

We also attempt to provide further insight into some controversial details of the electronic structure of these complexes of cobalt, such as the character of the highest occupied SCF orbital,[6] role of the metal 4*s* and 4*p* orbitals in the metal-carbon bond,[8,9] nature of the π backbonding,[8–11] the extent of error introduced through the Hartree–Fock overestimation of the metal–ligand bond lengths,[2–5,12] and the spin multiplicity[1,13] of $HCo(CO)_3$.

COMPUTATIONAL DETAILS

With few exceptions, calculations described here utilize the optimized geometries, reported in paper I. We label the trigonal bipyramidal (tbp) conformations according to the apical ligands: HC, CC, HV, and CV (letters denote hydrogen, carbonyl, or vacancy). The near-tetrahedral states are labeled according to their symmetry (C_{3v} or C_s) and electronic configuration. We continue to use the basis set described in paper I, which consists of a 12*s*7*p*4*d*, (33321/331/4) basis on the cobalt atom,[14,15] and of the 3-21G functions[16] on the light atoms. We refer to this as the small basis set.

We also introduce another basis set by replacing the cobalt *d* orbitals [DZC basis of Tatewaki and Huzinaga[14] with the split-valence set proposed by Hay[17] (the "augmented 4*d*" basis)]. This amounts to a 12*s*7*p*5*d* basis set, contracted as (33321/331/311). The Dunning–Hay 3*s*2*p* split valence basis[18] is used on the light atoms, augmented by Huzinaga's *d*-type polarization functions[15] on carbon and oxygen ($\alpha = 0.600$ and 1.154). To this basis were added diffuse *s*- and *p*-type functions,[19] using the exponents 0.036, 0.0438, and 0.0845 on hydrogen, carbon, and oxygen, respectively. This set is referred to as the large basis set.

All of the configuration-interaction calculations are limited to single and double excitations selected by perturbation theory, with the Hartree–Fock or CASSCF configurations as reference, and the Hartree–Fock (or CASSCF) and virtual *K* orbitals[20] as the basis. All energy values were extrapolated to the full CI limit by means of a variant of the CI extrapolation formula.[21] This extrapolation provides a degree of size consistency, which is necessary for any comparison of the energy of $HCo(CO)_4$ with that of the products of dissociation, $HCo(CO)_3$ and CO. We have performed three basic types of calculations:

Type (1) Hartree–Fock and CI calculations in the small basis, with 94 basis functions in $HCo(CO)_4$ and 76 functions in $HCo(CO)_3$. Uncorrelated core orbitals in the CI calculations include 1*s*,2*s*,2*p*,3*s* and 3*p* orbitals on the cobalt atom, 1*s* orbitals on carbon and oxygen, 3σ(CO) (the C–O σ bonds), and the 4σ(CO) orbitals (oxygen lone pairs). The entire virtual space was used for electron excitations.

Type (2) Hartree–Fock and CI calculations in the large basis, with 190 basis functions in $HCo(CO)_4$ and 152 functions in $HCo(CO)_3$. Core orbitals in the CI calculations include 1*s*, 2*s*, and 2*p* orbitals on the cobalt atom, and 1*s* orbitals on carbon and oxygen. The virtual space was truncated to 83 orbitals for $HCo(CO)_4$ and 68 orbitals for $HCo(CO)_3$. The calculation of this size could not be carried out for the C_{3v} conformation of $HCo(CO)_4$, due to limitations of the available CI programs.

Type (3) CASSCF/CI calculations in the small basis (76 functions) were performed for the near-tetrahedral trip-

 0021-9606/88/084967-12$02.10

let states of the molecule $HCo(CO)_3$. The active space consisted of four d-type tetrahedral hybrids, describing the two lone pairs and two unpaired d electrons. The total number of configurations in the MCSCF procedure was 6. This was followed by single- and double-excitation CI calculations, using the six configurations of the CASSCF as the reference. The occupied CASSCF orbitals, supplemented with K-type virtuals, were used as the basis for the CI calculations; the core included 1s, 2s, 2p, 3s, and 3p orbitals of cobalt, and the 1s orbitals on carbon and oxygen. The entire virtual space of 40 orbitals was used for electron excitations.

The software package MELD[22] was used to perform the large scale configuration-interaction calculations, and the MCSCF calculations were done with the program GAMESS.[23] All of the calculations were performed on a VAX 11/780, and an FPS 164 vector processor.

STRUCTURE OF THE TETRACARBONYL COMPOUND

We reported in paper I that the geometry optimization at the Hartree–Fock level predicts the existence of two tbp conformations of $HCo(CO)_4$, C_{3v} with H axial, and C_{2v} with H equatorial. The C_{2v} form has lower SCF energy (by 0.002 a.u.), contrary to the experimental findings.[24]

Using the Hartree–Fock orbitals of the closed-shell $^1A_1$ state of the C_{3v} conformation, we performed a CI calculation of type (1) for $^1A_1$. Two d^8 ^3E triplet states were also located: the lowest ^3E state has wave functions $(d_{x^2-y^2})^1(d_{z^2})^1$ and $(d_{xy})^1(d_{z^2})^1$, with the $(d_{xz})^1(d_{z^2})^1$ and $(d_{yz})^1(d_{z^2})^1$ pair of wave functions 0.018 a.u. above it. Detailed SCF and CI calculations of type (1) were performed on the lower triplet state. Several open-shell singlet states were also found, about 0.5 a.u. above the triplets, and were not investigated further.

Analogous calculations were performed at the experimental C_{3v} geometry, in order to assess the effects due to the Hartree–Fock elongation of the metal–ligand bonds. At the optimized C_{2v} geometry, calculations of types (1) and (2) were performed on the closed-shell $^1A_1$ state only.

Table I summarizes the energy values for $HCo(CO)_4$. The SCF energy of the closed-shell C_{3v} configuration increases at the shorter Co–C distances, compared to the longer SCF optimum bond length; but the CI energy decreases.

TABLE I. CI energies (a.u.) of the $HCo(CO)_4$ species.

State	Geometry[b]	E_{HF}	E_{extrap}[c]
$^1A_1$	C_{3v}	−1824.6297	−1825.2416
$^1A_1$	C_{3v},expt.[c]	−1824.6031	−1825.2618
$^1A_1$	C_{2v}	−1824.6318	−1825.2410
^3E[a]	C_{3v},$^1A_1$opt.	−1824.6594	−1825.2470
^3E	C_{3v},expt.	−1824.5801	−1825.2096
^1E	C_{3v},expt.	−1824.5101[d]	−1825.1560

[a]Configuration $(d_{z^2})^1(d_\epsilon)^1$.
[b]SCF optimized for the appropriate electronic state, if not specified otherwise.
[c]Experimental geometry, see Ref. 15.
[d]^1E was calculated with orbitals of the corresponding triplet state, ^3E.
[e]CI type (1).

This is a strong indication that electron correlation represents a major component in the metal–ligand bonding; similar conclusions were drawn elsewhere, on the basis of results reported for ferrocene and iron pentacarbonyl.[4,5]

The SCF energy of the ^3E state increases even more at shorter bond lengths, chiefly because of one unpaired electron in the a_1 orbital. Consequently, the CI energy is also increased by this bond compression. This situation can be diagrammed as follows for calculations of type (1):

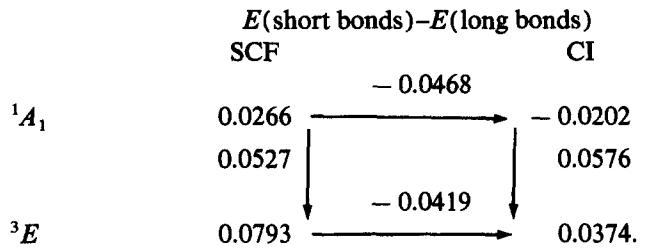

(1)

The differences along the horizontal arrows show the extent to which the change in electron correlations diminish the energy increase due to the shorter bonds. The values are fairly similar for the two states. Clearly dispersion forces, as represented by the change in electron correlation, are a major factor in determining ligand–metal bond energy and bond length.

At the optimized $^1A_1$ SCF geometry, Hartree–Fock calculations in the small basis place the ^3E state 0.029 a.u. below the closed-shell, d^3, $^1A_1$. This could be partially explained by the bias of the Hartree–Fock method towards open-shell states, but the CI calculation provides a correction of only 0.024 a.u. to the singlet–triplet gap, yielding a (still) unphysical result of a ^3E ground state. At the experimental geometry, the singlet lies below the lowest triplet at either level of calculation, and the correlation correction increases this singlet–triplet energy gap by 0.029 a.u. Hence the CI correction to the singlet–triplet gap is relatively independent of bond length. We summarize the singlet–triplet energy differences as follows for calculation of type (1):

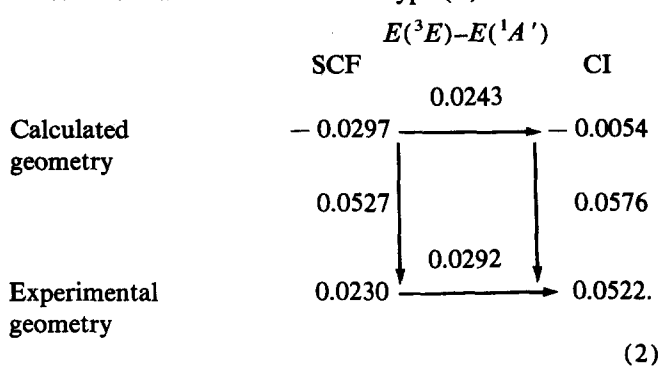

(2)

Consequently, the correlation correction is essential to predicting the correct ground state because it leads to shorter bond lengths for the singlet state, and not directly because of the higher correlation energy of the closed-shell system.

Finally, the Hartree–Fock calculations [type (1)] predict the C_{2v} conformation to be 0.002 a.u. more stable than the C_{3v}. CI calculations of type (1) do not enable us to draw a conclusive distinction between the energies of these two

TABLE II. Mulliken orbital populations on the cobalt atom of the $HCo(CO)_4$ species.

State	$^1A_1$	$^1A_1$	$^1A_1$	^3E
Geometry	C_{3v}	C_{3v},expt.	C_{2v}	C_{3v},expt.
SCF (small basis)				
3*d*	7.49	7.46	7.49	7.44
4*s*	0.13	0.05	0.18	0.05
4*p*	1.01	0.85	1.02	0.62

conformations (0.0006 a.u. in favor of C_{3v}). The correlation energy is similar for the two conformations at the optimized geometries: 0.610 a.u. for the C_{3v}, and 0.609 for the C_{2v}. This leads us to conclude that the postulated,[13] and experimentally corroborated,[24] greater stability of the C_{3v} must reflect the fact that, in the two conformations, the bond lengths are influenced to different extents by the electron correlation. However, it is not possible to account reliably for the bond length corrections in the C_{2v} conformation. No experimental data are available on the C_{2v} geometry, and, although the metal–carbon bond lengths of the C_{3v} form probably could be used in a model C_{2v} geometry, there is no knowledge of the correct length of the equatorial H–Co bond. The SCF pictures of the apical and equatorial H–Co bonds differ considerably, and the optimized axial bond length is 0.12 Å larger than the equatorial one (see Tables 1 and 3 in paper I). In the tbp complexes, the Hartree–Fock method elongates the axial bonds more than those in the equatorial positions.[1,12]

Type (2) CI calculations for the open-shell C_{2v} states ($^3B_1$ and $^1B_1$) were done with the orbitals of the closed-shell state. Therefore, the relative position of the two open-shell states is described reasonably well, and the singlet is located well above the corresponding triplet.

Mulliken orbital populations on the cobalt atom are listed in Table II. Although the populations are basis dependent (see paper I), certain trends are apparent. Formally, the cobalt is Co(I) d^8 in the valence bond description with five dsp^3 orthogonal hybrid orbitals used for forming coordinate covalent bonds to the ligands. Because of the way shared electron pairs are counted in a Mulliken population analysis, some of the d^8 electrons are lost by π "backbonding" while some dsp^3 population should be gained by σ bonding. At shorter bonds, the 4*sp* populations decrease in the SCF picture, as expected, because of the large diameter of these orbitals.[25]

Introduction of the larger basis set on cobalt increases the 3*d* population by 0.4, while decreasing the 4*p* population by the same amount. The electronic charge distribution around cobalt in the C_{2v} tetracarbonyl is $Co^{(0)}\ d^8(sp)^1$ in the large basis. The increased 3*d* contribution in the large basis is probably due to the greatly improved set of *d* functions used.

THE QUESTION OF π BACKBONDING, AND OTHER FEATURES OF THE METAL–LIGAND BONDS

The π-bonding model of Dewar, Chatt, and Duncanson[26] has been widely invoked as an explanation of a variety of features of the transition metal complexes. The model is remarkably successful as a qualitative concept, and we have demonstrated the existence of an unequivocal π interaction between the cobalt 3*d* shell, and a strong π acceptor, the ethylene ligand.[27] However, in the case of a weaker π acceptor, such as carbonyl, it is difficult to relate the idea of π backbonding to any physically demonstrable feature of the electronic structure.

Bagus and Roos[11] have analyzed CASSCF wave functions in terms of Mulliken populations, in order to demonstrate the π backbonding in the NiCO compound. Their analysis yields σ donation of 0.4 electrons, and π backdonation of 0.6 electrons. However, the dependence of the Mulliken populations on the basis set is well known. It is difficult to make a distinction between the physical phenomena and basis-set effects, especially in the presence of delocalized basis functions. At best, one can observe relative trends within the same orbital (or atom), but the conclusions based on comparisons of the absolute magnitudes of populations of the σ and π systems need independent corroboration.

The method of constrained space orbital variations (CSOV) was used by Bauschlicher and Bagus,[9] in a study of $Ni(CO)_4$ and $Fe(CO)_5$. This method allows for an independent evaluation of the energies of σ and π interactions and the above authors conclude that the π interaction is 3 times stronger than σ in the $Fe(CO)_5$ complex, and almost 20 times stronger in $Ni(CO)_4$.

This method does not measure the relaxations from the state of infinitely distant molecular fragments (i.e., the bonding energies), but the stepwise relaxations from a high-energy state, obtained by forcing the infinitely distant fragments together, while keeping their orbitals unchanged. The energy of relaxation from this state into the ground state is approximately twice as large as the dissociation energy, in both cases. The sum of energies attributed to the σ donation and π backdonation is 5.36 eV in the $Ni(CO)_4$, 1.83 eV more than the dissociation energy of 3.53 eV. In the case of $Fe(CO)_5$, the sum of σ and π relaxation energies is 9.08 eV, and the dissociation energy is 7.54 eV. The relative magnitudes of the σ and π components of CSOV relaxations reflect primarily the influence of the imposed variational constraints, and do not relate to the magnitudes of the much smaller σ and π components of the metal–ligand bond energy.

As the populations proved to be too dependent on the basis, we characterize the molecular orbitals qualitatively, by means of two- and three-dimensional contour maps of functional values (see also paper I).

In the SCF picture, π interaction between cobalt and the axial carbonyl in $HCo(CO)_4$ is contained in the fully occupied orbitals 7*e*, 9*e*, and 11*e*, whose *a'* components are shown in the small basis, at the experimental geometry, in Figs. 1 to 3. The π(CO) orbitals interact, both bondingly and antibondingly, with the d_{xz} and d_{yz} orbitals on cobalt (orbitals 7*e* and 9*e*). The d_{xz} and d_{yz} lone pairs, usually associated with electron donation into π^*(CO), feature a nodal plane through the carbon atom, and there are no occupied orbitals with distinct π^*(CO) character at all. This picture persists at different metal–ligand bond lengths, and in the large basis. Any π bonding between cobalt and the carbonyl would have

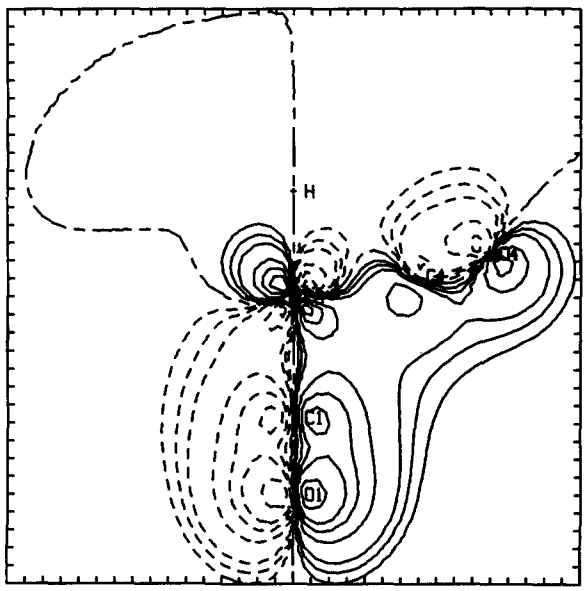

FIG. 1. 7*e* orbital of the C_{3v} conformation of $HCo(CO)_4$, at the experimental geometry, represented in the small basis set. Contours enclose 10%, 30%, 50%, 70%, 90%, 95%, and 98% of the electron density, and the orbital is plotted in one of the symmetry planes.

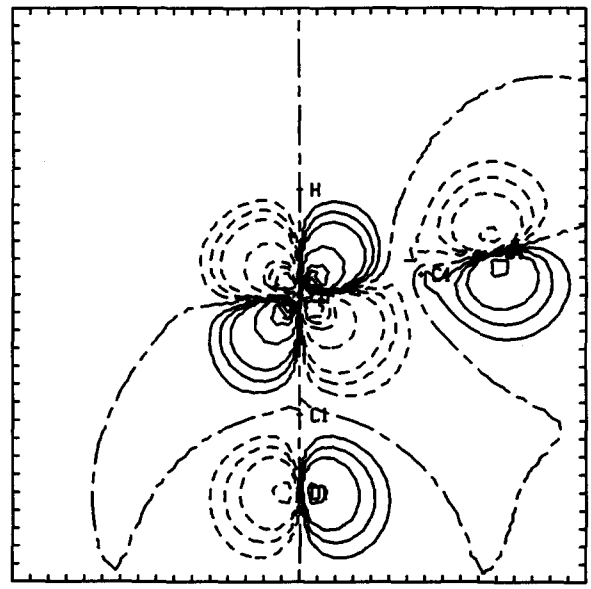

FIG. 3. 11*e* orbital of the C_{3v} conformation of $HCo(CO)_4$, at the experimental geometry, in the small basis.

to amount to a difference between the bonding and antibonding interactions. The σ bond, in contrast, is rather unequivocal (orbital 16 a_1). Although the comparison of the two types of bonds is entirely qualitative, the SCF picture does not confirm the conclusion of the Mulliken[11] analysis, to the effect that the σ and π bonds should be of comparable strength. Also, we cannot corroborate the overwhelming π character which the CSOV[9] method attributes to the metal–carbonyl bond in $Fe(CO)_5$ and $Ni(CO)_4$, complexes rather similar to the cobalt compounds discussed here.

As reported in paper I, the HOMO of the C_{3v} conformation of $HCo(CO)_4$, at the SCF-optimized geometry, has the character of an H–Co bond, rather localized on the hydrogen atom ($17a_1$, Fig. 4). At the experimental geometry, this orbital lies below the HOMO equatorial pair of metal *d* orbitals (12*e*, Fig. 5). This interchange is due to the increase in antibonding interaction, bringing the orbital picture into agreement with SCF-$X\alpha$-SW results.[6]

The much larger radius[25] of the 4*p* shell of cobalt, relative to 3*d*, a feature often forgotten in the qualitative discussions, is apparent in the pictures of the equatorial *d*-orbital set, 12*e*. The equatorial H–Co bond (orbitals $18a_1$ and $19a_1$ of the C_{2v} conformation), is delocalized over two molecular orbitals. Such bonding is possible because of the large differ-

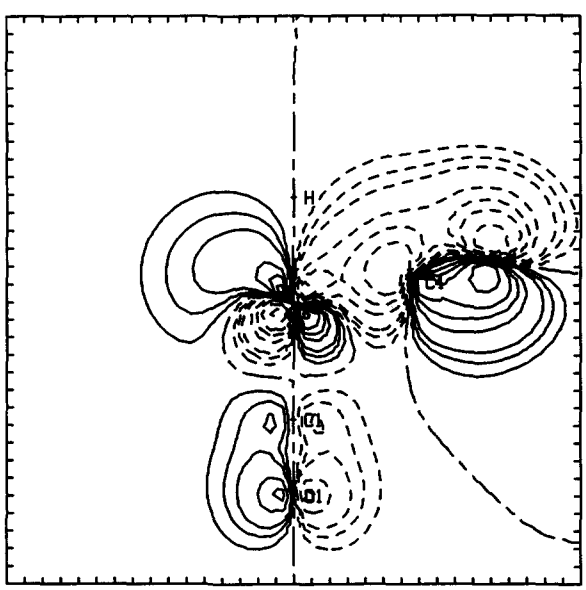

FIG. 2. 9*e* orbital of the C_{3v} conformation of $HCo(CO)_4$, at the experimental geometry, in the small basis.

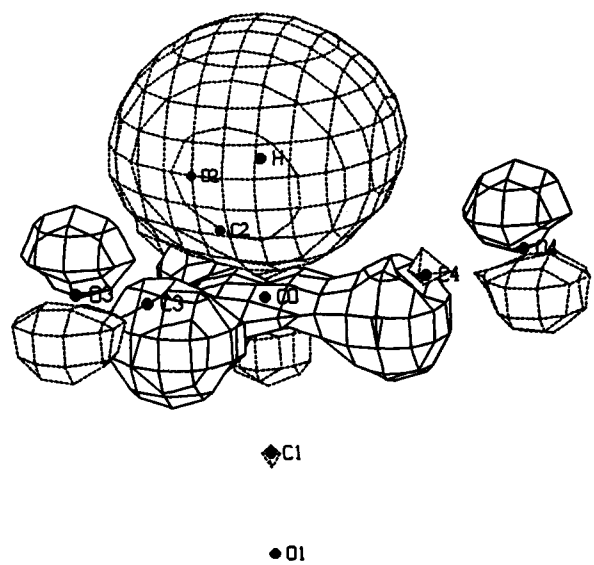

FIG. 4. $17a_1$ orbital of the C_{3v} conformation of $HCo(CO)_4$, at the experimental geometry, in the small basis. Contour encloses 90% of the electron density.

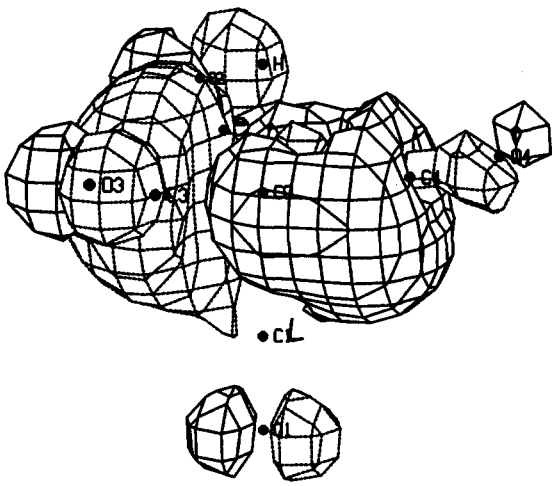

FIG. 5. 12*e* orbital of the C_{3v} conformation of $HCo(CO)_4$, at the experimental geometry, in the small basis.

ence in sizes of the 3*d* and 4*sp* shells, and is particularly prominent for the small hydrogen ligand.

By way of interpreting the infrared spectra of $HCo(CO)_4$, it has been hypothesized[28,29] that the hydrogen atom forms weak bonds to the equatorial carbons. There is indeed some overlap between hydrogen and the π_z orbitals on the equatorial carbonyls, in the orbital $15a_1$, but the corresponding antibonding in the hydride orbital $17a_1$ makes it difficult to estimate the net bonding effect.

TETRAHEDRAL TRIPLET STATES OF $HCo(CO)_3$

We have shown in paper I that the three lowest energy HF triplet states of hydridocobalt tricarbonyl have nearly tetrahedral geometries. We have found one state with the full C_{3v} symmetry, and two broken-symmetry states (C_s). The *d* orbitals in these states form five near-tetrahedral hybrids, one of which builds the Co–H bond, in the bonding–antibonding combination, similar to the equatorial tbp bonds. The remaining hybrids are labeled *e'*, *e"* (facing the edges) and *t'*, *t"* (facing the carbonyl vertices), primes indicating symmetry character under the vertical symmetry plane. We label the tetrahedral states by indicating the locations of the two unpaired electrons. The four remaining electrons occupy the hybrids not included in the label, e.g., the state $^3A_1$ $(e't' - e''t'')$ is an e^3t^3 two-configuration state whose wave function reads explicitly as $(e'')^2(t'')^2(e')^1(t')^1 - (e')^2(t')^2(e'')^1(t'')^1$. The electron configuration of the $^3A_2(t't'')$ state is shown below:

$$\begin{array}{ccc} & \sigma^*(\text{H–Co}) & \\ & -\uparrow-\downarrow- & \\ t' \quad -\uparrow- & & -\uparrow- \quad t'' \\ & -\uparrow-\downarrow- & \\ & \sigma(\text{H–Co}) & \\ e' \quad -\uparrow-\downarrow- & & -\uparrow-\downarrow- \quad e''. \end{array} \tag{3}$$

Exploratory CI calculations indicate that the orbitals of the H–Co bond remain doubly occupied in all states of interest, and that the active space consists of the six configurations having two holes in the "lone pair" hybrids. The near-tetrahedral states have C_{3v} or near-C_{3v} symmetry, and the one-configuration wave functions cannot describe all triplet states. Moreover, we must account for the first-order Jahn–Teller effect, to which the ^3E states are subject, and which opens the possibility of a broken-symmetry triplet ground state.

These conditions call for a geometry optimization at the MCSCF level. Such procedure was found to be too time consuming: instead, we have used the SCF optimized C_{3v} geometry of the nondegenerate, one-configuration state $^3A_2$ $(t')^1$ $(t'')^1$, as the prototype C_{3v} geometry (lowest triplet state of the ligand-field theory).

The Jahn–Teller distortions of the regular tetrahedron usually amount to elongations and contractions along the C_2 symmetry axes; of the two classes of states (oblate and prolate), one corresponds to minima on the energy surface, and the other to the saddle points of the pseudorotations which connect these minima. The SCF optimizations of the two $^3A'$ configurations $(e'')^2(t'')^2(e')^1(t')^1$ and $(e')^2(t')^2(e'')^1$ $(t'')^1$ provide two geometries which, respectively, correspond to the oblate and prolate distorted tetrahedra. These distortions are readily understood as the sterical accommodations of the unpaired electrons (see Table III, and also Table 15 in paper I for the full geometry). Linear combinations of the two $^3A'$ configurations constitute the $^3A_1$ and $^3E'$ wave functions of $HCo(CO)_3$ (Table IV and Fig. 6).

Single-point calculations of all three types were performed, at the near-tetrahedral geometries. SCF and CI cal-

TABLE III. Lengths of the sides of distorted tetrahedra of $HCo(CO)_3$ (Å).

State[a]	$^3A_2(t't'')$	$^3A'(e't')$	$^3A'(e''t'')$
Geometry	C_{3v}	oblate	prolate
H–C_x[b]	3.076	3.138	3.129
H–C_y[c]	3.076	3.140	3.154
C_x–C_y	3.200	3.151	3.464
C_y–C_y	3.200	3.715	3.217

[a]Configuration for which the SCF geometry optimization was carried out.
[b]Carbon atom in the symmetry plane.
[c]Carbon atom outside the symmetry plane.

TABLE IV. CI [type (3)] energies (a.u.) of the near-tetrahedral states of $HCo(CO)_3$.

Geometry	State[a]	E_{CASSCF}	E_{extrap}
C_{3v}	$^3A_2(t't'')$	−1712.6045	−1713.334
C_s, oblate	$^3A_2(t't'')$	−1712.5985	−1713.310
C_s, prolate	$^3A_2(t't'')$	−1712.5985	−1713.309
C_{3v}	$^3A_2(e't'' + e''t')$	−1712.5904	−1713.338
C_s, oblate	$^3A_2(e't'' + e''t')$	−1712.5919	−1713.357
C_s, prolate	$^3E'(e't' + e''t'')$	−1712.5927	−1713.352

[a] C_{3v} symmetry labels of the prolate and oblate states are only approximate. The labels E' and E'' denote the even and odd components of the near-E state.

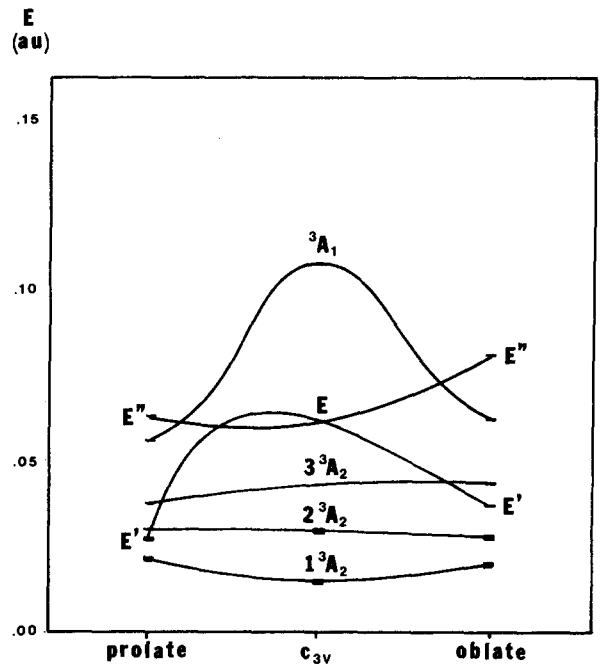

FIG. 6. Tetrahedral deformation of the triplet $HCo(CO)_3$. Orbitals of the heavily marked states were optimized in the CASSCF calculations.

culations of the types (1) and (2), which differ mostly in the size of the basis and of the core, present rather similar pictures of the single-determinantal states. The lowest state is the $^3A_2$ (t',t''), of the full symmetry. Of the two distorted states, the oblate tetrahedron is favored at the Hartree–Fock level, but the CI calculations yield lower energies for the prolate form.

In the calculations of type (3) shown in Tables IV and V, we have obtained optimized orbitals for the first two CI states. The CASSCF procedures on these states yield two sets of energies of the higher states, for each geometry. The lower of the two CI energies was chosen for each state, and a sketch of the CASSCF results on the tetrahedral deformation is shown in Fig. 6.

In addition to the first-order splitting of the E level, mixing with the higher $^3A_1$ state brings the E' component down, on the prolate side. On the oblate side, the state $^3A_2$ resides below both the $^3E'$ and $^3E''$ components. The state $^3A_2$ $(t't'')$ retains the lowest energy throughout the deformation, at the CASSCF level. The multireference CI calculation [type (3)] brings the states $^3E'$ and $^3A_2$ below the $^3A_2$ $(t't'')$, but the energy difference at the C_{3v} geometry is rather small, 0.0044 a.u. in favor of $^3A_2$ $(e't'' + e''t')$. At both C_s geometries, however, the two-configuration states lie distinctly below the lowest C_{3v} level. Although the procedure of type (3) becomes prohibitively costly in the large basis, single-configuration calculations indicate the change introduced by the improvement in the basis set. In the large basis, the energy of the C_{3v} $^3A_2$ $(t't'')$ state is lowered by 0.006 a.u. with respect to the single-configuration C_s states, whose relative energy changes by 0.0014 au. These changes are too small to reverse the ordering of C_{3v} and C_s states; the lowest triplet state of $HCo(CO)_3$ is a near-tetrahedral d^8 state of symmetry C_s. The two broken-symmetry states derive from the double-minimum state $^3A_2$ $(e't'' + e''t')$, and a splitting of the ^3E state. The CI calculation of type (3) favors the oblate tetrahedron by 0.0051 a.u. This difference is too small to ascertain which form represents the minimum on the energy surface.

PYRAMIDAL DEFORMATION OF THE C_{3v} FORM OF $HCo(CO)_3$

An EHT study by Elian and Hoffmann[13] indicates that the closed-shell $^1A_1$ state of a d^8, tetracoordinated C_{3v} carbonyl complex, has an energy minimum at the pyramidal angle of 90°, and that, when this angle increases beyond 100°, a $^3A_2$ state acquires lower energy than the $^1A_1$ state. At that value of the angle, a crossing occurs between the energy levels of the filled "t"-type d orbitals, and of an empty a_1 EHT orbital, with the predominant d_{z^2} character.

The SCF geometry optimizations in the small basis yield a C_{3v}, closed-shell state whose pyramidal angle is 90° (the conformation HV), and a $^3A_2$ state, with the angle of 114° [the fully symmetric near-tetrahedral state $(t')^1(t'')^1$], 0.105 a.u. below the former. Both states are SCF stable, i.e., their wave functions retain the C_{3v} symmetry, even if the calculations are performed without symmetry constraints. Calculations below used the geometries of these two states.

TABLE V. MCSCF energies[a] (a.u.) of the near-tetrahedral states[b] of $HCo(CO)_3$.

Geometry		C_{3v}		C_s, oblate			C_s, prolate	
$^3A_1$	0.4917	0.5147	$^3A_1$	0.5584	0.5160	$^3E''$	0.5580	0.5160
^3E	0.5450	0.5590	$^3E''$	0.5089	0.5400	$2\,^3A_2$	0.5907	0.5506
			$^3E'$	0.5833	0.5636	$^3A_1$	0.5140	0.5649
$3\,^3A_2$	0.5536	0.5776	$3\,^3A_2$	0.5726	0.5769	$3\,^3A_2$	0.5809	0.5831
$2\,^3A_2$	0.5742	0.5904	$2\,^3A_2$	0.5440	0.5919	$^3E'$	0.5580	0.5927
$1\,^3A_2$	0.6045	0.6028	$1\,^3A_2$	0.5985	0.5965	$1\,^3A_2$	0.5985	0.5956

[a] Underlined energies were obtained by orbital optimization. Energies of the other states in each column were obtained as roots of the 6×6 CI matrix, using the optimized orbitals of the underlined state. States $e'e''$ and $t't''$ retain the same relative position in every column. All entries should be preceded by the digits $-$ 1712 so that, for example, 0.4917 is to be read $-$ 1712.4917.

[b] The states are: $1\,^3A_2(t't'')$, $2\,^3A_2(e't'' + e''t')$, $3\,^3A_2(e'e'')$, $^3E(e't' + e''t'', e't'' - e''t')$, $^3A_1(e't' - e''t'')$.

Single-point SCF calculations for the $^1A_1$ and $^3A_2$ states were performed, with interchanged geometries. The resulting $^3A_2$ (90°) state is SCF stable, and is located 0.074 a.u. below $^1A_1$ (90°). The $^1A_1$ (114°) state was also found to be SCF stable, but marginally so. An SCF calculation without symmetry constraints upon the wave function, and using different initial orbitals, produces a wave function of symmetry C_s. This state is 0.0317 a.u. below the $^1A_1$ (114°) state of C_{3v} symmetry, and only 0.002 a.u. above the $^1A_1$ (90°); its proper geometry is that of the CV conformation.

The readiness of the SCF procedure to produce a low-lying C_s state, in addition to the C_{3v}, would not be easily distinguishable from the possible SCF instability of the latter state. Such discontinuous collapses of the symmetric SCF wave functions have little to do with the actual structure of the molecule; rather, they are the consequence of the fact that, while the exact eigenfunctions are invariant under the symmetry group of the Hamiltonian, their variational approximations need not be. An unstable SCF state indicates that the SCF variational space might not be wide enough to describe the energy profile of the pyramidal deformation. CI calculations of type (1) were performed on the four states, with the objective of decreasing the relative energy of the $^1A_1$ (114°) state without effectuating the collapse of the symmetry of the wave function. However, such a decrease did not occur, indicating that the $^1A_1$ (114°) state is SCF stable. Instead, the overall singlet–triplet energy gap decreased, as expected.

The $^3A_2$ (114°) state is virtually identical to the $^3A_2$ ($t't''$) MC state (see above), and has marginally higher energy than the $^3A_2$ ($e't' - e''t''$) state, in the type (3) calculations. Another type of $^3A_2$ SCF state was found, both at 90° and 114°. This type corresponds to the configuration $(e')^1(e'')^1$, although it can also be characterized as $(d_{xz})^1(d_{yz})^1$.

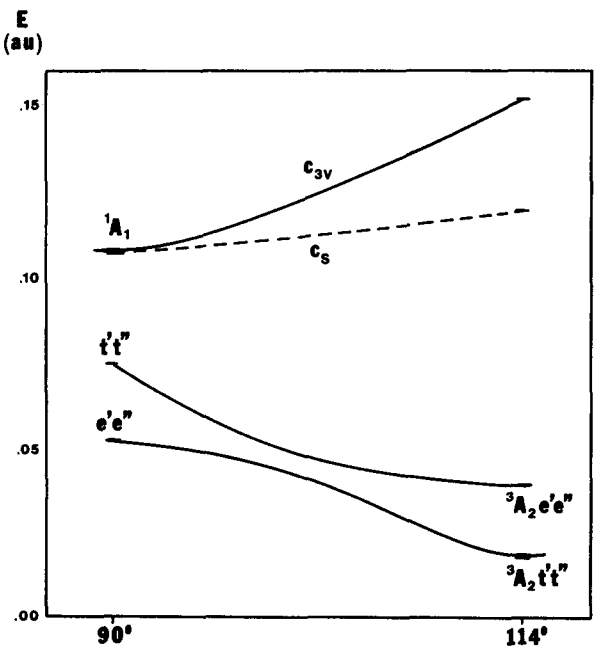

FIG. 7. Pyramidal deformation of the C_{3v} conformation of $HCo(CO)_3$, described at the SCF/CI level of type (1).

The tetrahedral hybrids are not as pronounced in this state as in the $^3A_2$ ($t't''$) and the 4p character of its unpaired electrons is much smaller. MC calculations show that these two states do not interact very strongly at the near-tetrahedral geometry (114°), despite their relative proximity (~0.020 a.u. of energy). At the SCF level, the $e'e''$ state lies above the $t't''$, but the CI calculation of type (1) interchanges their ordering at 90°. This is plausible, since the $e'e''$ wave function is really of the tbp type. An avoided crossing of the two $^3A_2$ levels must occur during the pyramidal deformation, but we do not know the full extent to which these two states interact at 90°. The change in the energy levels is shown in Fig. 7.

At the type (1) CI level, then, the $^3A_2$ (90°) states ($t't''$) and ($e'e''$), are seen to be 0.034 and 0.055 a.u. below the $^1A_1$ (90°) state, in disagreement with the EHT predictions. Since the geometry of the $^3A_2$(90°) states is only approximate, the gap between the states with optimized geometry must be even larger. On the other hand, the bond length correction increases the energy of the triplet states, relative to the singlets (see below). Short-bond calculations for the HC conformation show that the correction to the singlet–triplet gap is less than 0.010 a.u. Therefore, the occurrence of the singlet–triplet crossing in the pyramidal deformation, described in the EHT studies, could not be confirmed.

TRIGONAL BIPYRAMIDAL TRIPLET STATES OF $HCo(CO)_3$

As shown in paper I, three d^7p^1 triplet states, having approximate tbp geometries, occur in $HCo(CO)_3$. They are readily understood as excitations of an equatorial d electron into the directional receptor, mostly 4p in character, which was left behind after the departure of one carbonyl from $HCo(CO)_4$. The HC conformation gives rise to two such states, $^3A'$ and $^3A''$, which correspond to the excitations from the a' and a'' equatorial d orbitals. In the CC conformation, both equatorial d orbitals are of the a' type, one of them with substantial hydride character. The $^3A''$ states require energetically unfavorable excitations from the e''-type d orbitals, and we have found only the $^3A'$ state. SCF geometry optimizations in the small basis and CI calculations of type (1) were performed on these states (see Table VI). The lowest

TABLE VI. CI energies (a.u.) of the tbp open-shell $HCo(CO)_3$ species.

State	Geometry	E_{HF}	E_{extrap}	
$^3A'(d^7p^1)$	C_s(HC)	−1712.5611	−1712.9873	[Type (1)]
		−1714.6016	−1715.7417	[Type (2)]
$^3A'(d^7p^1)$	C_s(HC)	−1712.5426	−1712.9909	[Type (1)]
		−1714.5851	−1715.7627	[Type (2)]
$^3A''(d^7p^1)$	C_s(HC)	−1712.5599	−1712.9923	[Type (1)]
		−1714.6532	−1715.7658	[Type (2)]
$^3A''(d^7p^1)$	C_s(HC), s.b.	−1712.5396	−1713.0086	[Type (1)]
$^3A'(d^7p^1)$	C_s(CC)	−1712.5645	−1713.0166	[Type (1)]
		−1714.6492	−1715.7585	[Type (2)]
$^1A'(d^7p^1)$	C_s(CC)	−1712.5389[a]	−1712.9923	[Type (1)]
$^3A_2(t't'')$	C_{3v}(HV)	−1712.5723	−1713.0061	[Type (1)]
$^3A_2(e'e'')$	C_{3v}(HV)	−1712.5637	−1713.0279	[Type (1)]

[a] Calculated with orbitals of the corresponding triplet state, $^3A'$, C_s, CC.

energy of the CC, $^3A'$ state is understandable on sterical grounds, since the apical positions are more spacious than the equatorial ones. Regarding the HC states, the marginally lower energy of the $^3A''$ probably has to do with better separation of the unpaired electrons in the orbitals of different symmetry.

The d^7p^1 states in the HC and CC conformations are attributed to the fact that the $4sp$ receptor, facing the equatorial vacancy, has far lower energy than the empty d_{z^2} orbital, facing the two apical ligands (see paper I). An additional advantage of the d^7p^1 configuration lies in the large diameter of the $4p$ orbitals; this accomplishes the radial separation of the unpaired electrons.

The same rationale explains the absence of d^7p^1 states of the HV and CV conformations. In these cases, both d_{z^2} and $4p_z$ face only one ligand, and the d_{z^2} belongs to the shell of lower energy. In the tbp geometry, however, the configuration $(d_{z^2})^1(d_{e'})^1$ brings the unpaired electrons close together, because of the equatorial ring of the d_{z^2} orbital, and the tetrahedral coordination is preferable.

Single-point Hartree–Fock calculations in the large basis produce different results for the tbp triplets. In the type (2) calculations, two tbp d^8 triplets appear, $^3A'$ of the CC conformation, and $^3A''$ of the HC. These states can be interpreted as two different distortions of the lowest tetrahedral d^8 triplets, of the respective symmetries A_1 and A_2. The $^3A''$ state appears 0.002 a.u. below the tetrahedral $^3A_2$, in the type (2) calculation.

The conclusion drawn from this discrepancy between the results of calculations of types (1) and (2) is that the stability of the d^7p^1 triplets must be exacerbated by the nature of the small basis, which tends to improve upon the d shell by using the $4s$ and $4p$ functions. Nevertheless, it is reasonable to assume that these states exist as minima on the d^7p^1 surfaces, since true energy minima were found by the optimization in the small basis, and also on the ground of qualitative arguments. The four surfaces, characterized by the d^8 and d^7p^1 configurations, and by the symmetries A' and A'', all have energy values close to one another, and must undergo crossings and avoided crossings at certain geometries.

The lowest $^3A'$ state of the HC conformation in the large basis is a d^7p^1, despite the fact that, in the small basis, it has higher energy than the other two d^7p^1 states. The corresponding d^8 tbp state has the two unpaired electrons placed into d orbitals of the same symmetry, $d_{x^2-y^2}$ and d_{z^2}. This seems unfavorable enough to allow for the lowest $^3A'$ state to have the d^7p^1 configuration.

"SHORT-BOND" GEOMETRIES OF THE HC CONFORMATION OF $HCo(CO)_3$

In order to estimate the effect of excessively long metal–ligand bonds upon the structure of $HCo(CO)_3$, we have constructed approximate geometries for the HC conformation, which is similar to the C_{3v} conformation of hydridocobalt tetracarbonyl. Three states were examined: $^1A'$, $^3A'$, and $^3A''$. The SCF-optimized bond angles were used in all cases, and the bond lengths were constructed as follows: for the closed-shell $^1A'$ state, bond lengths of the experimental geometry[24] of the C_{3v} $HCo(CO)_4$ were used, and for $^3A'$ and $^3A''$ the difference of the theoretical lengths of triplet and singlet bonds was added to the experimental values for $HCo(CO)_4$. Such constructions are not reliable for the conformations CC and CV, since no experimental value exists for the length of the equatorial H–Co bond. The bond lengths for the closed shell state of the HV conformation can be constructed by analogy with $HCo(CO)_4$.

Results of the calculations of types (1) and (2) (Table VII) show the expected rise in the Hartree–Fock energy, and the decrease in the CI energy. Again, in order to obtain a good prediction of the bond lengths, geometry optimization must include correlation effects. At the Hartree–Fock level, the energy differences are fairly independent of the size of the basis set, in agreement with the results on ferrocene.[2–4] The configuration-interaction calculation of type (2) yields a larger decrease in energy than the type (1), especially for the $^3A'$ state.

In order to estimate the relative importance of geometry, basis set size and electron correlations, we compare the sizes of energy gaps between pairs of electronic states for the two types of geometry, at the SCF and CI levels of theory:

Type 1:

	$E(^3A')-E(^1A')$			$E(^3A'')-E(^1A')$		
	SCF		CI	SCF		CI
		0.0469			0.0408	
Long bonds	−0.0586	→	−0.0117	−0.0575	→	−0.0167
	0.0013	(0.0091)	0.0104	0.0032	(−0.0055)	−0.0023
		0.0560			0.0353	
Short bonds	−0.0573	→	−0.0013	−0.0543	→	−0.0190,

Type 2:

	SCF	$E(^3A')-E(^1A')$ CI
		−0.0070
Long bonds	−0.0177 →	−0.0107
	−0.0008 (0.0047)	0.0039
	0.0117	
Short bonds	−0.0185 →	−0.0068.

(4)

The results differ from those for $HCo(CO)_4$. Even though the singlet–triplet gap becomes fairly small at the short-bond geometry, after the correction for the Fermi correlation, the triplet state remains the lower of the two. Two-thirds of the correction in $HCo(CO)_4$ come from the decrease in the bond lengths (0.055 a.u.), most of it obtainable at the Hartree–Fock level. In the $HCo(CO)_3$ the geometry corrections are small and indistinct, since the equatorial vacancy allows for easier accomodation of the *d* electrons, and the 4*sp* hybrid is not very sensitive to the metal–ligand bond lengths. At the SCF level, the correction is larger for the $^3A''$ state, in which one unpaired electron faces the equatorial carbonyls.

Bond length energy differences show that the correlation components of the metal–ligand bonds are of the same order as in $HCo(CO)_4$:

Type 1:

	E(short bonds)−E(long bonds) SCF	CI		SCF	CI
		−0.0311			−0.0311
$^1A'$	0.0171 →	−0.0140	$^1A'$	0.0171 →	−0.0140
	0.0014	0.0104		0.0032	−0.0023
	−0.0221				−0.0366
$^3A'$	0.0185 →	−0.0036	$^3A''$	0.0203 →	−0.0163,

Type 2:

	SCF	CI
		−0.0422
$^1A'$	0.0173 →	−0.0249
	−0.0008	0.0039
	−0.0375	
$^3A'$	0.0165 →	−0.0210.

(5)

In the small basis, the SCF energy difference between the long- and short-bond geometries is larger than the CI difference. This observation is valid for all three states of the HC conformation. For the states $^1A'$ and $^3A'$, the bond length correction to the SCF energy changes insignificantly with the improvement of the basis set, by 0.0002 and 0.002 a.u., even though the basis was doubled (76 vs 152 functions). This result is in agreement with the findings of the studies on ferrocene, which show a similar insensitivity of the metal–ligand distances to the size of the basis.

CHARGE REDISTRIBUTION DUE TO THE ELECTRON CORRELATION, AND THE PROBLEM OF METAL–LIGAND BOND LENGTHS

A study of (η-ethylene)hydridocobalt tricarbonyl[27] shows that an insight into the problem of metal–ligand bond lengths can be gained by investigating the difference between the electron distributions of the correlated and Hartree–Fock wave functions. Second moments provide a convenient description of the general pattern of the distribution of electrons.

Table VIII shows the second electric moments of the electron distribution on the C_{3v} forms of tri- and tetra-carbonyl complexes. The moments are calculated in the principal axis frame, located at the center of the valence electronic charge; the core electrons and nuclear charges are not included in the results.

Comparison of the CI and SCF results shows that the effect of the electron correlation is to decrease the electric moments, rendering the charge distribution more compact. For $HCo(CO)_4$ and the HV conformation of $HCo(CO)_3$, the distribution of correlated electrons tends to be more ob-

TABLE VII. CI energies (a.u.) of the tbp open-shell $HCo(CO)_3$ species.

State	Geometry	E_{HF}	E_{extrap}	
$^1A'$	C_s(HC)	−1712.5024	−1712.9756	[Type (1)]
		−1714.5839	−1715.7310	[Type (2)]
$^1A'$	C_s(HC), s.b.[c]	−1712.4853	−1712.9896	[Type (1)]
		−1714.5666	−1715.7559	[Type (2)]
$^1A'$	C_s(CC)	−1712.5018	−1712.9767	[Type (1)]
		−1714.5829	−1715.7334	[Type (2)]
$^1A'$	C_s(CV)	−1712.5089	−1712.9844	[Type (1)]
		−1714.5678	−1715.6815	[Type (2)]
$^1A_1$	C_{3v}(HV),90°[d]	−1712.4989	−1712.9727	[Type (1)]
		−1714.5725	−1715.7210	[Type (2)]
$^1A_1$	C_{3v},[a] 114°	−1712.4650	−1712.9284	[Type (1)]
$^1A_1$	C_{3v},[b] 114°	−1712.4967	−1712.9610	[Type (1)]

[a]Wave function of C_{3v} symmetry, geometry of the state $^3A_2(t't'')$.
[b]Wave function of C_s symmetry, geometry of the state $^3A_2(t't'')$.
[c]Short bonds. See description in the text.
[d]Pyramidal angle.

late than that of the Hartree–Fock wave function. On the other hand, comparison of the type (1) and (3) CI distributions with the HF and CASSCF distributions of the near-tetrahedral $^3A_2(t't'')$ and $^3A_2(e't''-e''t')$ states, shows a small effect in the opposite direction.

In all cases, a withdrawal of charge takes place, from the periphery of the molecule, on the outer side of the hydrogen and oxygen atoms, and a buildup closer to the metal (see Fig. 8). In the tbp conformations, the withdrawal is stronger from the axial positions, and the buildup occurs in the equatorial plane. The apical hydrogen appears less "hydride-like" in the CI description, and the oblateness of the charge is increased. In the tetrahedral case, the redistribution is more isotropic, lacking the distinction between the apical and equatorial positions. Also, the "nonhydride" hydrogen undergoes a buildup of charge, rather than depletion, decreasing the oblateness in the tetrahedral cases.

In the studies of cobalt and manganese nitrosyls, Fenske and Jensen,[30] and also Bursten *et al.*,[31] have discussed the symmetry collapse of the SCF wave functions in molecular species of $C_{\infty v}$ symmetry. The CI methodology restores much of the symmetry of the wave functions, and the latter authors conclude that the electron correlation leads to greater sphericity of the charge distribution. Aside from the increased compactness of the charge, our results do not argue in favor of more isotropic CI distributions. Rather, the changes in the relative sizes of second moments appear to be dependent on the overall geometry of the molecule.

We have also calculated the electrostatic forces,[27] exerted upon the nuclei by the differential distribution of the electronic charge, $\rho_{CI}-\rho_{SCF}$. These forces indicate the magnitude and direction of the correlation correction to the SCF-optimized geometry. It must be understood that the magnitude of the force reflects changes in both length and strength of the bond.

Forces on the carbon atoms indicate that the correlation leads to smaller metal–carbonyl distances, in all cases. The metal–hydrogen bond, however, is somewhat harder to account for. Calculations of type (1), on the C_{3v} form of $HCo(CO)_4$, show that all single excitations must be included into the CI matrix, for the force on the apical hydrogen to point toward cobalt. At the same time, the forces on the oxygen atoms, pointed towards carbon, grow disproportionately large, indicating a shortening of the C–O bonds. This runs against the fact that the SCF method underestimates the C–O bond length (see paper I, Table 1). Calculations of type (2), in the large basis set, and with all single excitations included, were performed on the closed-shell states of the HC and HV conformations of $HCo(CO)_3$, and yielded a contraction of the Co–C bonds, an elongation of the C–O bonds, and a smaller outward pull on the apical hydrogen.

Calculations of type (3), performed on the near-tetrahedral states, in the small basis, show that the inclusion of all single excitations does not yield the inward-directed force on hydrogen.

TABLE VIII. Principal second moments of the distribution of correlated electrons of the C_{3v} conformations of $HCo(CO)_4$ and $HCo(CO)_3$ (a_0^2 with respect to the center of valence electrons).

	$HCo(CO)_4$	$HCo(CO)_4$	$HCo(CO)_3$	$HCo(CO)_3$	$HCo(CO)_3$	$HCo(CO)_3$
	Calc. Geom.	Expt. Geom.	HV,$^1A_1$	$^3A_2(t't'')$	$^3A_2(t't'')$	$^3A_2(e't''+e''t')$
Calc. type	1	1	2	1	3	3
Electrons	34	34	48	28	40	40
SCF wave function[a]						
$\langle r^2-3z^2\rangle$	76.40	78.12	743.94	285.50	596.22	595.24
$\langle r^2\rangle$	678.92	639.18	889.23	502.82	858.24	859.00
CI wave function						
$\langle r^2-3z^2\rangle$	78.30	79.76	743.20	283.25	593.26	591.72
$\langle r^2\rangle$	676.08	639.59	888.10	500.35	854.97	855.72

[a]CASSCF wave function in calculations of type (3).

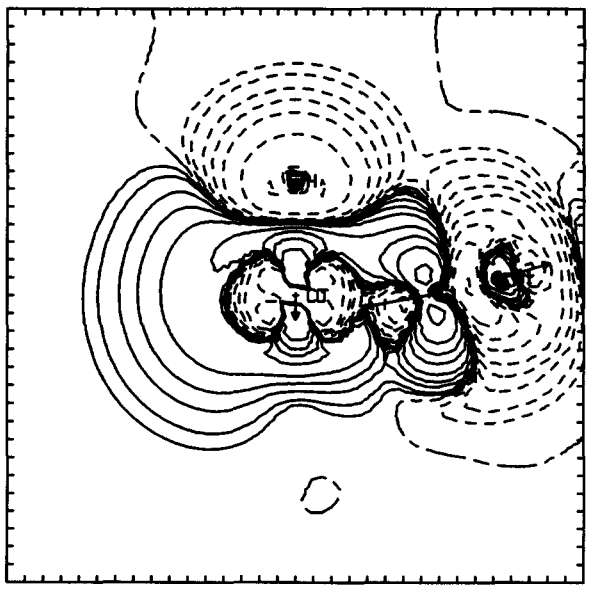

FIG. 8. Density difference of the $^1A_1$ state of the HV conformation of $HCo(CO)_3$, at the optimized geometry, in the large basis; plotted in the symmetry plane.

The $\pi \rightarrow \pi^*$ (and $\sigma \rightarrow \sigma^*$) correlations of the carbonyls elongate the C–O bond. Similarly, diminished charge density between the cobalt and carbon atoms, due to the $\sigma \rightarrow \sigma^*$ correlations, elongates the Co–C bonds. However, there is a buildup of charge along the tbp axis, close to the cobalt atom, and in the areas corresponding to the d–π^* overlap in the π-bonding model. These increases appear to offset the usual bond elongation, brought about by electron correlation. As we have shown, it is exceedingly difficult to attribute an unambiguous physical quantity to the cobalt–carbonyl π bonding. The π-like buildup of charge corresponds most tangibly to an off-axis interaction, accounted for only at the CI level, and offers an explanation for the failure of the SCF method to yield correct bond lengths. Similarly, the axial buildup on cobalt explains the larger pull upon the axial carbonyl, and the larger SCF error in the length of axial bonds.

THE QUESTION OF THE GROUND STATE OF HYDRIDOCOBALT TRICARBONYL

The $HCo(CO)_3$ species turns out to be rather elusive, and the experimental evidence, although not entirely conclusive, indicates that small amounts of it could be found in equilibrium with $HCo(CO)_4$. No experimental data are available, concerning the nature of the electronic ground state of $HCo(CO)_3$, presumably because of its low stability, and because of the interfering presence of several other unstable cobalt carbonyl species (see references in paper I).

As we have shown above, two factors tend to decrease the SCF energy of triplet states, relative to the closed-shell state: Fermi correlation and excessively long bonds in the SCF-optimized geometries. When corrections are made for both of these factors, correct ordering of states is achieved in the C_{3v} $HCo(CO)_4$ molecule, with the ^3E state 0.0522 a.u. above the closed-shell singlet. Such reordering does not obtain for the HC conformation of $HCo(CO)_3$, in which the best available ground state remains a triplet.

Comparison of the type (1) energies shows that, on the closed-shell singlet surface, departure of one carbonyl from the C_{3v} $HCo(CO)_4$ is an endothermic process, requiring 0.0447 a.u. of energy for the formation of the low-energy CV conformation of $HCo(CO)_3$, in the long-bond geometry. The dissociation into the HC conformation requires 0.0535 a.u., and the correction of the bond lengths increases the endothermicity to 0.0597 a.u.

To summarize, the calculations of type (1), (2), and (3) provide strong evidence for a triplet ground state of $HCo(CO)_3$, probably of the broken-symmetry tetrahedral type (see Table IV). In the catalytic cycle of hydroformylation, the hydridocobalt tricarbonyl (and other tetracoordinated intermediates) are postulated to undergo complexations with carbon monoxide, alkene or the hydrogen molecule (see references in papers I and II). These complexations, which involve transfer of an electron pair onto the cobalt atom, are facilitated by the presence of an empty directional receptor in the closed shell states. Partial occupation of that receptor in the d^7p^1 triplet states, or its absence in the tetrahedral states, hinders the complexation. Moreover, should all tetracoordinated species have triplet ground states, the catalytic cycle would have to consist of repeated transitions from the singlet to triplet surface and back.

Two modifications to the postulated hydroformylation mechanism could be suggested, in order to keep the reaction on the singlet surface. Either the removals and acquisitions of ligands have a high degree of simultaneity, which does not allow the tetracoordinated intermediate species to be formed, or (analogously) the reversible, noncatalytic complexations occur between the catalytic steps, keeping the intermediate species in pentacoordinated, closed-shell forms.

Correct prediction of the metal–ligand bond lengths is a major theoretical bottleneck at this point, since no reliable ordering of the energy levels of different multiplicity can be achieved without it. Use of the experimental geometries, when such are available, usually produces plausible qualitative results, but it is not known to what extent this geometry constraint influences the relative energies of the electronic states.

As shown in the study of iron pentacarbonyl[5], and here, electron correlation introduces the right correction into the Hartree–Fock optimized geometry, but the nature of the minimum reference space required for the full bond-length correction is not known. As we have shown, the single-reference calculations already yield a significant improvement in the description of the metal–carbonyl bond, as well as an insight into the nature of the CI correction. It is probable, however, that the quantitatively correct picture would require full MCSCF geometry optimizations, in a reference space which includes the orbitals of the Dewar–Chatt–Duncanson model. Unlike the Hartree-Fock calculations, we expect such calculations to be sensitive to the choice of the

basis set, especially in the description of the stretching frequencies of the metal–ligand bond.

ACKNOWLEDGMENT

This work was supported by the National Science Foundation under Grant No. CHE-85-03415.

[1]D. Antolovic and E. R. Davidson, J. Am. Chem. Soc. **109**, 977 (1987).
[2]H. P. Luthi, J. Ammeter, J. Almlof, and K. Korsell, Chem. Phys. Lett. **69**, 540 (1980).
[3]H. P. Luthi, J. H. Ammeter, J. Almlof, and K. Faegri, J. Chem. Phys. **77**, 2002 (1982).
[4]J. Almlof, K. Faegri, B. E. R. Schilling, and H. P. Luthi, Chem. Phys. Lett. **106**, 266 (1984).
[5]H. P. Luthi, P. E. M. Siegbahn, and J. Almlof, J. Phys. Chem. **89**, 2156 (1985).
[6]C. J. Eyermann and A. Chung-Phillips, J. Am. Chem. Soc. **106**, 7437 (1984).
[7]C. J. Eyermann and A. Chung-Phillips, J. Chem. Phys. **81**, 1517 (1984).
[8]P. S. Bagus, K. Hermann, and C. W. Bauschlicher, J. Chem. Phys. **80**, 4378 (1984).
[9]C. W. Bauschlicher and P. S. Bagus, J. Chem. Phys. **81**, 5889 (1984).
[10]C. W. Bauschlicher, S. P. Walch, and S. R. Langhoff (private communication).
[11]P. S. Bagus and B. O. Roos, J. Chem. Phys. **75**, 5961 (1981).
[12]J. Demuynck, A. Strich, and A. Veillard, Nouv. J. Chim. **1**, 217 (1977).
[13]M. Elian and R. Hoffmann, Inorg. Chem. **14**, 1058 (1975).
[14]H. Tatewaki and S. Huzinaga, J. Chem. Phys. **71**, 4339 (1979).
[15]*Gaussian Basis Sets for Molecular Calculations*, edited by S. Huzinaga (Elsevier, New York, 1984), p. 24.
[16](a) J. S. Binkley, J. A. Pople, and W. J. Hehre, J. Am. Chem. Soc. **102**, 939 (1980); (b) M. S. Gordon, J. S. Binkley, J. A. Pople, W. J. Pietro, and W. J. Hehre, *ibid.* **104**, 2797 (1982).
[17]P. J. Hay, J. Chem. Phys. **66**, 4377 (1977).
[18]T. H. Dunning and P. J. Hay, *Modern Theoretical Chemistry*, edited by H. F. Schaefer III (Plenum, New York, 1976), Vol. 3.
[19]T. Clark, J. Chandrasekhar, G. W. Spitznagel, and P. von Rague Schleyer, J. Comp. Chem. **4**, 294 (1983).
[20]D. Feller and E. R. Davidson, J. Chem. Phys. **74**, 3877 (1981).
[21]E. R. Davidson, in *The World of Quantum Chemistry*, edited by R. Daudel and B. Pullman (Reidel, Dordrecht, 1974).
[22]L. McMurchie, S. Elbert. S. Langhoff, and E. R. Davidson, MELD, subsequently modified by D. Feller and D. Rawlings.
[23]M. Dupuis, D. Spangler, and J. J. Wendoloski, GAMESS, subsequently modified by M. Schmidt and S. Elbert for the FPS 164.
[24]E. A. McNeille and F. R. Scholer, J. Am. Chem. Soc. **99**, 6243 (1977).
[25]S. P. Walch and C. W. Bauschlicher, in *Comparison of Ab Initio Quantum Chemistry with Experiment for Small Molecules*, edited by R. J. Bartlett (Reidel, Dordrecht, 1985).
[26](a) M. J. S. Dewar, Bull. Soc. Chim. Fr. **18**, C 71 (1951); (b) J. Chatt and L. A. Duncanson, J. Chem. Soc. **1953**, 2939.
[27]D. Antolovic and E. R. Davidson, J. Am. Chem. Soc. **109**, 5828 (1987).
[28]W. F. Edgell, C. Magee, and G. Gallup, J. Am. Chem. Soc. **78**, 4185 (1956).
[29]W. F. Edgell and G. Gallup, J. Am. Chem. Soc. **78**, 4188 (1956).
[30]R. F. Fenske and J. R. Jensen, J. Chem. Phys. **71**, 3374 (1979).
[31]B. E. Bursten, J. R. Jensen, D. J. Gordon, P. M. Treichel, and R. F. Fenske, J. Am. Chem. Soc. **103**, 5226 (1981).